# Lakes_CCI+ - Phase 2
# D2.4. Algorithm Development Plan (ADP)

**Reference CCI-LAKES2-0014-ADP**

**Issue 2.1.1 – 17/10/2023**

Contract number: 4000125030/18/I-NB –Lakes_cci

**Non-public document**

11 rue Hermès, Parc Technologique du Canal — 31520 Ramonville Saint-Agne, France
Tel +33 (0)5 61 39 47 00 Fax +33(0)5 61 75 10 14
www.cls.fr

## CHRONOLOGY OF ISSUES

| Issue | Legacy Issues | Date | Objective | Written by |
|---|---|---|---|---|
| 1.0 | 1.0 | 19/03/2020 | Initial Version | S. Simis, JF Crétaux, H Yésou, E Malnes, H Vickers, P Blanco, C Merchant, L Carrea, C Duguay, Y Wu |
| | 1.1 | 24/04/2020 | Revision following ESA review | See above |
| | 2.0 | 30/07/2020 | LSWT MODIS data processing | C Merchant |
| | 2.1 | 29/09/2020 | Revision following ESA review | JF Crétaux, C Merchant, H Yésou, E Malnes |
| 2.x | 2.2 | 02/05/2022 | Updates accompanying CRDP v2.0 and v2.0.1 | X Liu, JF Crétaux, L Carrea, C Duguay, S Simis |
| | 2.3 | 06/07/2022 | Revision following ESA review | B. Calmettes |
| 2.1 | - | 06/09/2023 | Revision and updates accompanying CRDP v2.1.0, outlook towards CRDP v3.0.0 | S. Simis, B Calmettes, JF Crétaux, X Liu, A Mangili, H Yésou, L Carrea, C Duguay, Y Wu |
| 2.1.1 | | 17/10/2023 | Revision following ESA review | S. Simis, B Calmettes, JF Crétaux, X Liu, A Mangili, H Yésou, L Carrea, C Duguay, Y Wu |

Note: prior to document issue 2.1, the PVASR and ADP were provided in a combined document. From v2.1 onwards the two documents are provided separately and versioning is kept consistent with the CRDP release cycle.

| | | |
|---|---|---|
| Checked by | Stefan Simis – PML<br>J-F Cretaux - LEGOS | Stefan Simis<br>Jean-francois Cretaux |
| Approved by | Alice Andral - CLS | A. Andral |
| Authorized by | Clément Albergel - ESA | Clement Albergel |

## DISTRIBUTION

| Company | Names | Email |
|---|---|---|
| ESA | Clément Albergel | clement.albergel@esa.int |
| BC | Carsten Brockman | carsten.brockmann@brockmann-consult.de |
| BC | Dagmar Müller | dagmar.mueller@brockmann-consult.de |
| BC | Jorrit Scholze | jorrit.scholze@brockmann-consult.de |
| BC | Kerstin Stelzer | kerstin.stelzer@brockmann-consult.de |
| BC | Martin Boettcher | martin.boettcher@brockmann-consult.de |
| BC | Olaf Danne | olaf.danne@brockmann-consult.de |
| CLS | Alice Andral | aandral@groupcls.com |
| CLS | Anna Mangilli | amangilli@groupcls.com |
| CLS | Beatriz Calmettes | bcalmettes@groupcls.com |
| CLS | Nicolas Taburet | ntaburet@groupcls.com |
| CLS | Christophe Fatras | cfatras@groupcls.com |
| CLS | Pierre Thibault | pthibaut@groupcls.com |
| CNR | Claudia Giardino | giardino.c@irea.cnr.it |
| CNR | Mariano Bresciani | bresciani.m@irea.cnr.it |
| CNR | Monica Pinardi | pinardi.m@irea.cnr.it |
| CNR | Marina Amadori | amadori.m@irea.cnr.it |
| CNR | Rossana Caroni | caroni.r@irea.cnr.it |
| CNR | Giulio Tellina | tellina.g@irea.cnr.it |
| H2O Geo | Claude Duguay | claude.duguay@h2ogeomatics.com |
| H2O Geo | Yuhao Wu | mark.wu@h2ogeomatics.com |
| H2O Geo | Jaya Sree Mugunthan | jayasree.mugunthan@h2ogeomatics.com |
| H2O Geo | Justin Murfitt | justin.murfitt@h2ogeomatics.com |
| HYGEOS | François Steinmetz | fs@hygeos.com |
| LEGOS | Jean-François Cretaux | jean-francois.cretaux@cnes.fr |
| LEGOS | Paul-Gérard Gbektom | paul.gerard.gbetkom@legos.obs-mip.fr |
| PML | Stefan Simis | stsi@pml.ac.uk |
| PML | Xiaohan Liu | liux@pml.ac.uk |
| PML | Nick Selmes | nse@pml.ac.uk |
| PML | Mark Warren | mark1@pml.ac.uk |
| Sertit | Hervé Yésou | Herve.yesou@unistra.fr |
| Sertit<br>Sertit | Jérôme Maxant<br>Sabrina Amsil | maxant@unistra.fr<br>s.amzil@unistra.fr |
| Sertit | Rémi Braun | remi.braun@unistra.fr |
| UoR | Chris Merchant | c.j.merchant@reading.ac.uk |
| Bangor | Iestyn Woolway | iestyn.woolway@bangor.ac.uk |
| UoR | Laura Carrea | l.carrea@reading.ac.uk |
| UoS | Dalin Jiang | dalin.jiang@stir.ac.uk |
| UoS | Evangelos Spyrakos | evangelos.spyrakos@stir.ac.uk |
| UoS | Ian Jones | ian.jones@stir.ac.uk |

## LIST OF CONTENTS



## LIST OF TABLES AND FIGURES

# 1 Introduction

This Algorithm Development Plan (ADP) is not for public distribution..

The ADP details for each Lakes_CCI ECV:

- Algorithm developments planned to feature in CRPD v3.0. Examples include updates to models, classification codes, and algorithm training or calibration, at any processing level.
- Priorities for future algorithm developments beyond the next annual cycle.

For the LWE, LWLR, LSWT, LIC and LIT, the existing validation and the identified issues are developed in Product Validation and Algorithm Selection report (PVASR v 2.1.1) and not resume here.

# 2 Lake Water level - LWL

## 2.1 Candidate algorithms for LWL

The algorithm for LWL calculation is incorporated in the Hysope code, developed at LEGOS and detailed in the ATBD, and operates at CLS in the framework of the Hydroweb database. A version for non-operational use also runs at LEGOS and is based on the same equations but using Geophysical Data Records (GDRs) (delivery delay = 90 days) instead of IGDRs (delivery delay 1 to 2 days) (Cretaux et al., 2016).

The procedure is run against data within a priori defined polygons of lake contours (using the common dataset of maximum water extent outlines created for Lakes_cci) which are then processed using the Hysope software which is classically using the following equation:

$$LWL = Alt - Rcorr - TE \qquad [2.1]$$

Where LWL is considered with respect to a geoid, Rcorr is the measured range between the satellite and the lake surface, Alt is the altitude of the satellite above an ellipsoid and TE is the combination of all correction factors to take into account atmospheric refraction (propagation in the ionosphere and the troposphere), tidal effects (solid Earth, lake and polar), and geoid height above the ellipsoid. For readers who needs more detailed information a full discussion of the computation of LWL is found in Cretaux et al. (2009).

All corrections are released in the GDRs or the IGDRs. The range is chosen from different retracking considering that generally the OCOG retracking is the most suitable for continental surface (see E3UB v2.1.1 document). The geoid correction is calculated using the repeat track technique (see E3UB v2.1.1 and Cretaux et al. 2009, 2016).

## 2.2 Validation results for LWL

The general algorithm used to calculate water level over lakes is well known and established in scientific literature. To address the issues that are listed in the following sections, we need to analyse lakes where reference in situ data are available. Examples of these procedures are given in Ricko et al. (2012) and Arsen et al. (2015), comparing different lake databases.

Lakes_cci cooperates with the State Hydrological Institute of St Petersburg, which provides in situ data of LWL for a set of Russian and central Asian lakes. We also use existing databases on the web to increase the number of lakes that can be used for this purpose.

The comparative analysis allows the statistically best performing retracking algorithm to be selected, as has been widely demonstrated for lakes as well as rivers.

Additional metrics to validate the LWL products include comparison of individual LWL retrieval to the long-term LWL variability, to detect outliers. The impact of removing outliers is traced as part of this process.

## 2.3 Identified issues for LWL

There are two main issues currently under investigation for the processing of altimetry data over lakes. The first is related to the onboard tracking system, and the second is related to the processing of altimetry over small lakes.

We have identified solutions to address onboard tracking issues based on new a priori information. For retrieval of LWL over small lakes we identify solutions based in new algorithms for SAR data. Both approaches are detailed in section 2.4.

Another separate consideration of retrieval performance is the calculation of relative biases when several satellites of different types of orbits are used over a given lake. When we use a series of satellites such as Topex / Poseidon, Jason-1/2/3, we collect data from the same orbit, so that the relative bias between each mission is well described and calibrated (see Cretaux et al. 2009, 2011, 2013, 2018, Bonnefond et al. 2018). When observations from different orbit are used, however, such as with Jason and Envisat or Jason and Sentinel-3, another bias is added. The instrumental biases are known, but since the tracks do not cover the same position over the lake, an additional bias due to geoid error must be considered. A very simple method was developed at LEGOS to correct for this additional bias. The LWL is calculated independently using each track, over the whole period, and during the overlapping period we interpolate the point measurement from each pass and calculate the average difference between all interpolate points. It then corresponds to the additional bias due to geoid errors.

## 2.4 Future improvements for LWL

We have planned three main future improvements.

1. The LWL time series are based on long term time series of altimetry data. To achieve this goal, we process measurements from several satellites when it is possible. Currently the Topex / Poseidon, and Jason-1 are processed using only classical retracking based on the algorithm tuned for ocean-type waveform. For many lakes it is therefore not precise enough to be included in the products. The issue particularly concerns small and medium size lakes. In coordination with other projects and in accordance with the Hydroweb development plan, the waveform of these two satellites will be reprocessed using the so called OCOG retracking algorithms used for other missions and which gives better accuracy of the LWL time series. We expect to, first, increase the number of lakes within the database, and then to produce longer time series for existing lakes where only Envisat or Jason-2 / Jason-3 were processed. Length of time series of LWL is indeed essential in the framework of climate change studies, to detect climate signal within time series constrained by different types of periodic and non-periodic fluctuations.
2. From another project also funded by ESA (FDR4ALT), CLS developed a new approach on old missions like Envisat or ERS-2 to better analyse the quality of the level-2 altimetry data (range, atmospheric corrections, backscatter). The objective is to have a better editing selection of measurements that are finally used in the calculation of LWL and to filter out spurious data in a more suitable manner than what was classically done. First results of this method are encouraging us to continue in this direction for these old mission (before altimeters are switched onto SAR mode with the sentinel ones). Several (~100) new time series using Envisat data (from 2002 to 2010) have already been calculated, validated, and uploaded in Hydroweb and will contribute to increase the number of lakes in the CCI database.
3. Recent missions such as Sentinel-3 provide SAR data. One of the main advantages is to improve the spatial resolution of the altimeter along the track. Using unfocused SAR processing techniques, the resolution is improved by an order of magnitude compared to previous altimeters. It allows small-scale features over lakes and rivers to be captured more frequently and more accurately, particularly when their orientation is perpendicular to the satellite track. In 2021 a new approach based on physical simulations considering the lake contour and the instrument characteristics has been analysed. The new algorithm developed at CNES and LEGOS for this purpose is call LPP (Lake Physical Processing). Fitting the simulation on the waveforms gives the water height. The algorithm has been tested on the sentinel-3A and Sentinel-3B time series over very small lakes in south of France and in Switzerland. Using in situ measurements we have shown that this new approach has allowed to gain a factor of 2 to 5 in terms of accuracy, compared to the classical data processing using retracking algorithm (Boy et al., 2022). We plan to use this new algorithm on small lakes with the sentinel missions for lakes where the current results are too noisy to be inserted within the CCI database so far.

.

## 2.5 LWL References

Arsen, A., JF. Cretaux, and R. Abarca-Del-Rio. 2015. Use of SARAL/AltiKa over mountainous lakes, intercomparison with Envisat mission J. of Adv. Space Res. The Saral/ALtiKa satellite Altimetry Mission, 38, 534-548, 2015, doi: 10. 1080/01490419. 2014. 1002590

Bonnefond, P. ; Verron, J. ; Aublanc, J. ; Babu, K. N. ; Berge-Nguyen, M. ; Cancet, M. ; Chaudhary, A. ; Cretaux, J-F. ; Frappart, F. ; Haines, BJ. , Laurain, O. ; Ollivier, A. ; Poisson, JC. ; Prandi, P. ; Sharma, R. ; Thibaut, P. ; Watson, C. The benefits of the Ka-Band as evidenced from the SARAL/AltiKa Altimetric mission: quality assessment and unique characteristics of AltiKa data, Remote Sensing. 2018, 10(1), 83, doi:1039/rs/10010083

Boy F., Cretaux J-F., Boussaroque M., & Tison C., 2022, Improving Sentinel-3 SAR mode procesisng over lake using numérical simulations, IEEE Transactions on Geoscience and Remote Sensing, 60, 1-18, Art no. 5220518, doi: 10.1109/TGRS.2021.3137034

Cretaux, J. F., S. Calmant, V. Romanovski, et al. 2009. An absolute calibration site for radar altimeters in the continental domain: lake Issykkul in Central Asia, Journal of Geodesy 83 (8) 723-735 DOI: 10. 1007/s00190-008-0289-7

Cretaux, J. F., S. Calmant, V. Romanovski, et al. 2011 Absolute Calibration of Jason radar altimeters from GPS kinematic campaigns over Lake Issykkul, Marine Geodesy, 34 : 3-4, 291-318, DOI: 10. 1080/01490419. 2011. 585110

Crétaux J-F., Bergé-Nguyen M., Calmant S., Romanovski V. V., Meyssignac B., Perosanz F., Tashbaeva S., Arsen A., Fund F., Martignago N., Bonnefond P., Laurain O., Morrow R., Maisongrande P., 2013 Calibration of envisat radar altimeter over Lake Issykkul, J. Adv. Space Res., Vol 51, 8, 1523-1541, doi: 10. 1016/j. asr. 2012. 06. 039

Cretaux J-F, M. Bergé-Nguyen, S. Calmant, N. Jamangulova, R. Satylkanov, F. Lyard, F. Perosanz, J. Verron, A. S. Montazem, G. Leguilcher, D. Leroux, J. Barrie, P. Maisongrande and P. Bonnefond, 2018, Absolute calibration / validation of the altimeters on Sentinel-3A and Jason-3 over the lake Issykkul, Remote sensing, 10, 1679, ; doi:10. 3390/rs10111679

Egido A., and W. H. F Smith, 2017, Fully Focused SAR altimetry: Theory and Applications, IEEE, 55, 1

Ričko M., C. M. Birkett, J. A. Carton, and J-F. Cretaux, Intercomparison and validation of continental water level products derived from satellite radar altimetry, J. of Applied Rem. Sensing, Volume 6, Art N°: 061710, DOI: 10. 1117/1. JRS. 6. 061710, 2012

# 3 Lake water extent - LWE

## 3.1 Candidate algorithms for LWE

Based on inter-comparison on a small set of lakes with increasingly complex hydromorphology, an approach based only on optical HR imagery was previously adopted to generate the LWE product. Water surfaces are extracted from images based on the exploitation of an in-house processing chain (Figure 1), named ExtractEO (Maxant et al, 2022). This software suite is also in use for Copernicus EMS, and for the supply of "water surface" reference plans for SWOT CalVAL globally.

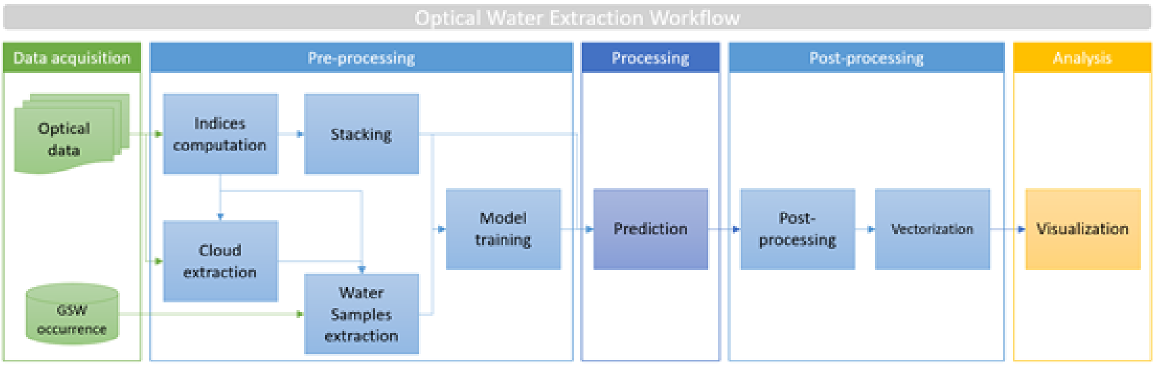


*Figure 1: Optical Water Extraction Workflow*

The preprocessing steps correspond to:

- Region Of Interest (ROI) is defined including the target lake.
- Selection of set of images representative of the different water levels of the target.
- Indices generation ‘AWEI, NDWI, MNDWI, NDI, SWIS which is a combination of indices)

The processing then follows the scheme shown in Figure 2:

- Automatic water sample generation from Global Surface Water. Water indices are computed to remove outliers and filter the training samples to the hydrological reality of the image (water extent, resolution)
- Training using the Multi-Layer Perceptron classifier (optionally a Support Vector Machine (SVM) or Random Forest (RF) approach can be applied)
- Slope and hillshade thresholds derived from HR DEMs are applied to refine the water extraction (post-processing)
- Minimum mapping unit (MMU) sieving to remove small features (0,1 hectares in this case)
- Water extent (in km$^2$) is subsequently calculated using the sum of individual pixel classified as water pixel within the ROI
- Generation of a max extent water mask

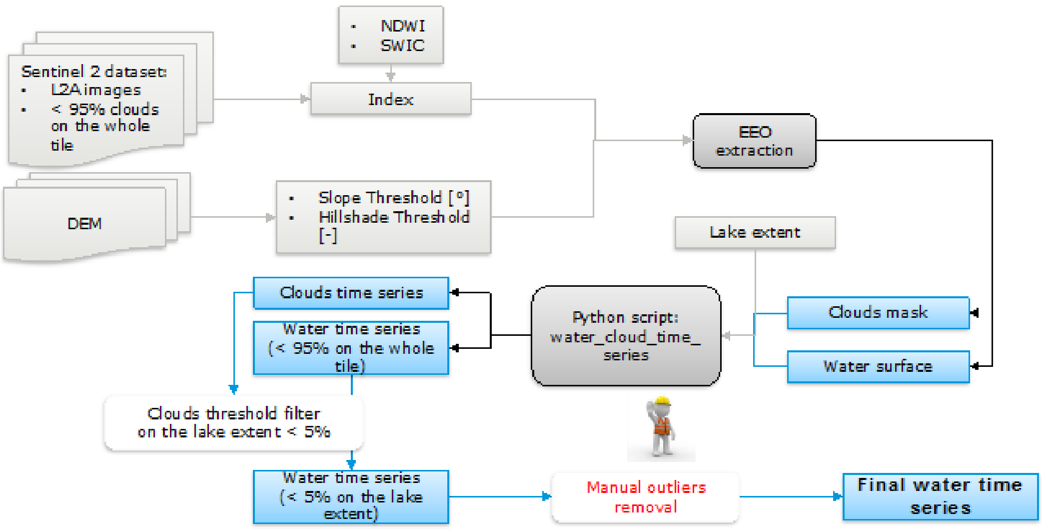


*Figure 2: Detailed workflow of the water extraction procedure within ExtractEO*

## 3.2 Future improvements for LWE

The method using SVM on optical imagery appears to provide a reliable and consistent approach despite sensitivity to cloud cover, and to a lesser degree, sunglint.

The presence of sunglint on water surfaces can disrupt the process of recognising and extracting water bodies (Gao et la., 2023). The appearance of this phenomenon depends not only on the position of the sun, but also on the location of the target in the swath. In order to limit re-treatments (Harmel et al., 2018; Tavares et al., 2021) it would be beneficial to develop a sunglint flag. This would allow automatic adjustment of relevant coefficients and thresholds in the ExtractEO processing chain.

Concerning cloud coverage, refinement of the existing cloud detector in the ExtractEO chain to provide a better cloud detection on the S2 L2A product, would be beneficial. This could be based in Machine Learning. The improved detection of clouds mask could be compared furthermore with such ancillary data as the SAFE mask from Colorado Boulder University or the Idepix procedure used within LWLR product generation. To address (small) cloud gaps, common water occurrence maps in databases such as GWS (Pekel et al. 2016) or GLAD (Pickens et al., 2022) might prove useful.

## 3.3 LWE References

Gao B-C, Li R-R. 2323. A Multi-Band Atmospheric Correction Algorithm for Deriving Water Leaving Reflectances over Turbid Waters from VIIRS Data. Remote Sensing. 2023; 15(2):425. https://doi.org/10.3390/rs15020425

Harmel T., Chami M., Tormos Th, Reynaud N., Danis P.A., 2018.Sunglint correction of the Multi-Spectral Instrument (MSI)-SENTINEL-2 imagery over inland and sea waters from SWIR bands, Remote Sensing of Environment, 204, 308-321, https://doi.org/10.1016/j.rse.2017.10.022.

Maxant J, Braun R, Caspard M, Clandillon S. (2022). ExtractEO, a Pipeline for Disaster Extent Mapping in the Context of Emergency Management. Remote Sensing. .14(20):5253. https://doi.org/10.3390/rs14205253

Pekel JF, Cottam A, Gorelick N, Belward AS. 2016.High-resolution mapping of global surface water and its long-term changes. Nature. 2016 Dec 15;540(7633):418-422. doi: 10.1038/nature20584.

Pickens, A.H., Hansen, M.C., Stehman, S.V., Tyukavina, A., Potapov, P., Zalles, V., Higgins, J. (2022) Global seasonal dynamics of inland water and ice. Remote Sensing of Environment, Volume 272, 112963

Tavares M.H., Lins R.C., Harmel T., Fragoso C.R. Jr., Martínez J.M., Motta-Marques D.,2021. Atmospheric and sunglint correction for retrieving chlorophyll-a in a productive tropical estuarine-lagoon system using Sentinel-2 MSI imagery, ISPRS Journal of Photogrammetry and Remote Sensing, 174, 215-236, https://doi.org/10.1016/j.isprsjprs.2021.01.021.

# 4 Lake surface water temperature - LSWT

## 4.1 Candidate algorithms for LSWT

Surface temperatures from infrared observations are obtained by coefficient-based methods or optimal estimation (OE, Merchant and Embury 2014). Because of the varied altitudes of lakes and the large differences in atmospheric absorption associated with continentality, optimal estimation is the appropriate approach for LSWT estimation (MacCallum and Merchant, 2012).

OE also provides comprehensive equations for uncertainty evaluation, on which basis uncertainty estimates are provided in LSWT products per datum.

As well as retrieval, classification of which pixels are filled with water under clear skies is a necessary part of the LSWT processing. This is done by a “fuzzy logic” style approach in which several metrics with fuzzy thresholds are combined into a “water detection score” that contributes to the definition of the quality level attributed to the pixel. Bayesian cloud detection, as used for sea surface temperature, was also considered to identify clear-sky pixels but is heavily compromised in its current implementation for small lakes, where the spatial coherence of the temperature of the scene is not a good indicator of cloud (unlike in the centre of large lakes and over open ocean). Because of the user requirement to increase the number of measured lakes, the latter scheme is therefore currently inapplicable for the identification of clear-sky only water pixels.

## 4.2 Future improvements for LSWT

For version LSWT v5.0 (Lakes_cci v3):

1. Inter-sensor consistency: The CDR will be made from seven sensors (2 ATSRs, MODIS, 2 AVHRRs and 2 SLSTRs) which have similar channels and nadir spatial resolution. Biases between sensor observations of a given lake arise because of relative calibration errors between sensors. Two steps will be applied. (New for v3.0) Calibration adjustments applied to brightness temperature. We are able to take advantage of bias-aware optimal estimation parameters obtained for AVHRRs within SST CCI (using plentiful ocean in situ data as an in-flight calibration reference). While not tuned for lakes, these will nonetheless reduce over-lake calibration biases.
2. Including night-time observations: This is a high-risk high-reward objective given the number of sensors, the subtlety required for nighttime detection of clouds, and the small amount of funded effort for the attempt. Nonetheless, without guaranteeing success, Bayesian cloud detection (adapted again from SST CCI) will be applied on nighttime observations, based on developing a new climatology of LSWT from the CDR v2.0/2.1. If validation of the nighttime results justifies their inclusion in v3.0, this will approximately double the observation frequency for some lakes (not necessarily all).
3. LSWT v5.0 will use ERA-5 for background numerical weather prediction information (except the lake surface water temperature which will be the climatology from CDR v2.1).

Beyond LSWT v5.0:

1. TRISHNA, which is planned to be launched in 2024, will offer measurements that are unique for LSWT coverage, quality and especially resolution, allowing to retrieve LSWT for smaller lakes with a higher frequency than the current high-resolution instruments which have low revisiting time (more than 15 days).
2. The U. S. successor to MODIS and AVHRR is the VIIRS series, which will be excellent for LSWT coverage and quality. VIIRS data will be available at CEDA as a lite version and therefore potentially it would be very interesting to attempt to retrieve LSWT from VIIRS which offer a better resolution (700m) than the classic meteorological satellites.

# 5 Lake water leaving reflectance - LWLR

## 5.1 Candidate algorithms for LWLR

Significant progress has been made in recent years in the field of water quality parameter retrieval, thanks to the extended operational period of OLCI (Ocean and Land Colour Instrument). New algorithms, ranging from machine-learning-based to semi-analytical and empirical approaches, have been developed. However, there remains a crucial need for an independent validation of water quality algorithms specifically designed for the OLCI sensor. In many cases, the same algorithms can still be applied to the Medium Resolution Imaging Sensors (MERIS), which was the focus of the previous algorithm selection and tuning exercise for sensors with this waveband set. For MODIS-Aqua, an algorithm selection and tuning exercise was completed in the previous version (2.x) of the Lakes_CCI.

To address the need for algorithm re-evaluation for OLCI/MERIS, we anticipated comprehensive algorithm validation to feed into better optimised solutions in CRDP v3.0. This validation process will involve not only the inclusion of selected algorithms currently implemented in Lakes_cci but also a collection of new algorithms targeting OLCI, published in recent years.

A summary of the candidate algorithms for Chla and Turbidity/TSM relating to OLCI is given in Table 1.

*Table 1: Summary of candidate new Chla algorithms for OLCI*

| Algorithm | Architectural approach | Formular | Original training (mg.m-3) | reference |
|---|---|---|---|---|
| OC4_OLCI | Blue-green ratios | MBR=Rrs(443>490>510)/Rrs560 | 0.01 to 78 | O'Reilly and Werdell 2019 |
| OC5_OLCI | Blue-green ratios | MBR=Rrs(413>443>490>510)/Rrs560 | 0.01 to 78 | O'Reilly and Werdell 2019 |
| OC6_OLCI | Blue-green ratios | MBR=Rrs(413>443>490>510)/M(560&665) | 0.01 to 78 | O'Reilly and Werdell 2019 |
| OC4_MERIS | Blue-green ratios | MBR=Rrs(442>490>510)/Rrs560 | 0.01 to 78 | O'Reilly and Werdell 2019 |
| OC5_MERIS | Blue-green ratios | MBR=Rrs(412>442>490>510)/Rrs560 | 0.01 to 78 | O'Reilly and Werdell 2019 |
| OC6_MERIS | Blue-green ratios | MBR=Rrs(412>442>490>510)/M(560&665) | 0.01 to 78 | O'Reilly and Werdell 2019 |
| Optimized QAA for OLCI | Semi-analytical | 1. Modified reference band ( ) of 709 or 754 nm in QAA Step 3: If MCI≤0.0016 choose 709 nm, else 754 nm<br>2. Modified equation and $\eta$ value in QAA Step 7 | 5 to 100 | Liu et al. 2020 |
| MDN | Machine learning | Mixed Density Network | 0.2 to 1209 | Pahlevan, Smith et al. 2020, Pahlevan, Smith et al. 2021, Smith, Pahlevan et al. 2021 |
| Bayesian | Bayesian probabilistic neural networks | Bayesian Neural Network | 0.05 to 68 | Werther et al. 2022 |
| Smith18 | Switched blending (G2B, OCI) | G2B algorithm refers to Gilerson, Gitelson et al. (2010). OCI algorithm refers to combined CI (Chl<0.25) and OC4E (Chl>0.25) algorithms. | 0.43 to 309 | (Smith, Lain et al. 2018) |

*Table 2: Summary of candidate new Turbidity/TSM algorithms for OLCI*

| Algorithm | Architectural approach | Formular | Original training (g.m-3) | reference |
|---|---|---|---|---|
| SOLID20 | MDN-based bbp inversion | Classification based | 0.1 to 2626.8 | Balasubramanian et al. 2020 |
| Jiang21 | Semi-analytical | Classification based | 0.09 to 2627 | Jiang et al. 2021 |
| Novoa21G | Switch blending | Linear-Green (TSM<10), Linear-Red (TSM 10~50), Poly-NIR (TSM>50) | 2.6 to 1579.1 | Novoa et al. 2017 |
| Novoa21B | Switch blending | Linear-Green (TSM<10), Nechad et al. (2010) NIR (TSM 10~50), Nechad et al. (2010) NIR (TSM>50) | 17.8 to 340.6 | Novoa et al. 2017 |
| Uudeberg20-clear | Band ratios | | 0.5 to 215.2 | Uudeberg et al. 2020 |
| Uudeberg2020-moderate | Band ratios | | 0.5 to 215.2 | Uudeberg et al. 2020 |
| Uudeberg20-Turbid | Band ratios | | 0.5 to 215.2 | Uudeberg et al. 2020 |
| Uudeberg20-VeryTurbid | Band ratios | | 0.5 to 215.2 | Uudeberg, et al. 2020 |
| Uudeberg20-Brown | Band ratios | | 0.5 to 215.2 | Uudeberg et al. 2020 |
| ANTA21 (Turbidity) | (based on Nechad 2009, tuned for OLCI) | T(red) was used if RW(red) < 0.05, and T(NIR) if RW(red) > 0.07, with a linear blending in the transition. Red=665 nm, NIR=865 nm | 0.83 to 176 FNU | Nechad et al. 2009, Dogliotti, et al. 2015, Klein, et al. 2021 |

*: ATA21 algorithm was developed for Turbidity

## 5.2 Future improvements for LWLR

As part of the Lakes_cci initiative, a new Calimnos processing chain is currently being developed, which includes anticipated updates in Idepix and Polymer. This update is expected to enhance the efficiency of LWLR processing, a requirement for any large-scale archive reprocessing in future.

The updated Idepix is faster with OLCI and includes improved ice flagging. The forthcoming release of Polymer (v4.17) which is being assessed incorporates experimental processing modes specifically designed for OLCI in complex coastal and highly turbid inland waters. This version also includes several performance improvements, which are necessary due to the longer run-time associated with the enhanced application range of the algorithm.

The Polymer upgrade encompass several key enhancements. Firstly, there is an optional parameterization of mineral absorption switching for Chl>10. Secondly, the first guess has been updated to test multiple initialisation points across the cost function, improving stability. Lastly, the inclusion of SWIR bands of 1020 for OLCI in bands_corr and bands_oc further improves algorithm stability.

It is expected that the upgraded version of Polymer offers a solution to the issue of unrealistic spectral shapes with visible discontinuities across optical gradients, which has been a significant challenge in extremely turbid regions with previous product versions. Once a conclusive evaluation of the Polymer version update is reached, a comprehensive LWLR data reprocessing can be initiated. In that case, all downstream water quality algorithms would require further validation and recalibration using the updated atmospheric correction results.

## 5.3 LWLR References


Balasubramanian, S. V., N. Pahlevan, B. Smith, C. Binding, J. Schalles, H. Loisel, D. Gurlin, S. Greb, K. Alikas and M. Randla (2020). Robust algorithm for estimating total suspended solids (TSS) in inland and nearshore coastal waters. Remote Sensing of Environment **246**: 111768.

Dogliotti, A. I., K. Ruddick, B. Nechad, D. Doxaran and E. Knaeps (2015). A single algorithm to retrieve turbidity from remotely-sensed data in all coastal and estuarine waters. Remote sensing of environment **156**: 157-168.

Gilerson, A. A., A. A. Gitelson, J. Zhou, D. Gurlin, W. Moses, I. Ioannou and S. A. Ahmed (2010). Algorithms for remote estimation of chlorophyll-a in coastal and inland waters using red and near infrared bands. Optics Express **18**(23): 24109-24125.

Jiang, D., B. Matsushita, N. Pahlevan, D. Gurlin, M. K. Lehmann, C. G. Fichot, J. Schalles, H. Loisel, C. Binding and Y. Zhang (2021). Remotely estimating total suspended solids concentration in clear to extremely turbid waters using a novel semi-analytical method. Remote Sensing of Environment **258**: 112386.

Klein, K. P., H. Lantuit, B. Heim, D. Doxaran, B. Juhls, I. Nitze, D. Walch, A. Poste and J. E. Søreide (2021). The Arctic Nearshore Turbidity Algorithm (ANTA)-A multi sensor turbidity algorithm for Arctic nearshore environments. Science of Remote Sensing **4**: 100036.

Liu, G., L. Li, K. Song, Y. Li, H. Lyu, Z. Wen, C. Fang, S. Bi, X. Sun and Z. Wang (2020). An OLCI-based algorithm for semi-empirically partitioning absorption coefficient and estimating chlorophyll a concentration in various turbid case-2 waters. Remote Sensing of Environment **239**: 111648.

Nechad, B., K. Ruddick and G. Neukermans (2009). Calibration and validation of a generic multisensor algorithm for mapping of turbidity in coastal waters. Remote Sensing of the Ocean, Sea Ice, and Large Water Regions 2009, SPIE.

Novoa, S., D. Doxaran, A. Ody, Q. Vanhellemont, V. Lafon, B. Lubac and P. Gernez (2017). Atmospheric corrections and multi-conditional algorithm for multi-sensor remote sensing of suspended particulate matter in low-to-high turbidity levels coastal waters. Remote Sensing **9**(1): 61.

O'Reilly, J. E. and P. J. Werdell (2019). Chlorophyll algorithms for ocean color sensors-OC4, OC5 & OC6. Remote sensing of environment **229**: 32-47.

Pahlevan, N., B. Smith, C. Binding, D. Gurlin, L. Li, M. Bresciani and C. Giardino (2021). Hyperspectral retrievals of phytoplankton absorption and chlorophyll-a in inland and nearshore coastal waters. Remote Sensing of Environment **253**: 112200.

Pahlevan, N., B. Smith, J. Schalles, C. Binding, Z. Cao, R. Ma, K. Alikas, K. Kangro, D. Gurlin and N. Hà (2020). Seamless retrievals of chlorophyll-a from Sentinel-2 (MSI) and Sentinel-3 (OLCI) in inland and coastal waters: A machine-learning approach. Remote Sensing of Environment **240**: 111604.

Smith, B., N. Pahlevan, J. Schalles, S. Ruberg, R. Errera, R. Ma, C. Giardino, M. Bresciani, C. Barbosa and T. Moore (2021). A chlorophyll-a algorithm for Landsat-8 based on mixture density networks. Frontiers in Remote Sensing **1**: 623678.

Smith, M. E., L. R. Lain and S. Bernard (2018). An optimized chlorophyll a switching algorithm for MERIS and OLCI in phytoplankton-dominated waters. Remote Sensing of Environment **215**: 217-227.

Uudeberg, K., A. Aavaste, K.-L. Kõks, A. Ansper, M. Uusõue, K. Kangro, I. Ansko, M. Ligi, K. Toming and A. Reinart (2020). Optical water type guided approach to estimate optical water quality parameters. Remote Sensing **12**(6): 931.

Werther, M., D. Odermatt, S. G. Simis, D. Gurlin, M. K. Lehmann, T. Kutser, R. Gupana, A. Varley, P. D. Hunter and A. N. J. R. S. o. E. Tyler (2022). A Bayesian approach for remote sensing of chlorophyll-a and associated retrieval uncertainty in oligotrophic and mesotrophic lakes. **283**: 113295.

# 6 Lake Ice cover – LIC

## 6.1 Candidate algorithms for LIC

The candidate algorithm remains the random forest (RF) classifier and the development plan therefore focusses on improvements to the classification accuracy.

As an ensemble approach, RF integrates decision trees developed by bagging samples to improve the limitations of the single-tree structure (Breiman, 2001). The bagging creates several subsets randomly from training samples with replacement (i.e. a sample can be collected several times in the same subset whereas other samples are probably not selected in this subset). Subsequently, each data subset is used to train a decision tree. For building a single tree, a random sample with several variables is chosen as split candidates from all variables. The number of variables available to a split is one of key RF hyperparameters, denoted as mtry. For the whole RF model, the number of trees (ntree) is defined a priori to develop various independent classifier outputs. The final class of each unknown sample is assigned by the majority vote of all outputs from the trees.

RF has been found to outperform threshold-based approaches (e.g., NASA Snow product), two other machine learning algorithms (multinomial logistic regression, MLR, and support vector machine, SVM) and to provide comparable results to gradient boosting trees (GBT) for lake ice cover, open water and cloud classification (Wu et al., 2021). Training, testing and validation of the MLR, SVM, GBT and RF algorithms from 17 lakes and ice seasons across the northern hemisphere found that RF with a combination of visible, near infrared, and mid infrared bands was the best choice for LIC product generation; more specifically, MODIS Terra/Aqua Level 1B calibrated radiances product (MOD02/MYD02), Collection 6.1 (TOA reflectance data) stored in two separate files as a function of spatial resolution: MOD02QKM/MYD02QKM (250 m, bands 1-2) and MOD02HKM/MYD02HKM (500 m, bands: 3-4, 6-7). While RF and GBT provided similar results following a comprehensive accuracy assessment (cross validation (CV): random k-fold as well as spatial and temporal CV), the former was selected for LIC product generation since it was determined to be less sensitive to the to the choice of hyperparameters necessary for classification compared to GBT, MLR and SVM. High overall accuracy (>95%) has been achieved with the RF classifier in both spatial and temporal transferability assessments (Wu et al., 2021).

## 6.2 Future improvements for LIC

As with any lake product generated from optical data, the presence of clouds as well as extensive cloud cover periods and low solar illumination angles, particularly during the fall freeze-up at high latitudes, introduce classification errors and limit the retrieval of open water and ice cover for many days of the year. In LIC v2.1, highly turbid lakes or sections of lakes have been found to occasionally be misclassified as ice-covered during the open water season. This is also the case for a few lakes that are characterized by snow-free blue clear ice during spring break-up; here ice is misclassified as open water. Also, one limitation of the LIC product is that no retrieval is performed when the solar zenith angle is >85 degrees; a limitation due to the use of MODIS shortwave bands that record very low surface reflectance during ice formation late fall and wintertime.

Given the above limitations, future improvements of the RF classifier and its related processing chain leading to the release of CRDP v3.0 will include:

(1) Enhancement of classification accuracy (product quality) via collection of a more extensive training dataset than that used in previous algorithm versions
(2) provision of better uncertainty estimates (pixel-level estimation of aleatoric, epistemic and total uncertainty; Saberi et al., in prep.) and quality flags beyond simple overall class accuracy reported in earlier CRDP releases

(3) revised label (class) aggregation, beyond the simple majority-vote approach currently used, from multiple satellite overpasses to daily product based on outcomes of (1) and (2).

## 6.3 LIC References

Breiman, L. (2001). Random forests. *Machine Learning*, 45(1), 5–32. doi: 10.1023/A:1010933404324.

Saberi, N., C.R. Duguay, E. Hüllermeier, K.A. Scott, and M. H. Shaker (In preparation). Uncertainty estimation of lake ice cover maps from a random forest classifier using MODIS TOA reflectance data.

Wu, Y., Duguay, C.R. & Xu, L. (2021). Assessment of machine learning classifiers for global lake ice cover mapping from MODIS TOA reflectance data. *Remote Sensing of Environment*, 253, 112206, doi: 10.1016/j.rse.2020.112206.

# 7 Lake Ice Thickness- LIT

## 7.1 Candidate algorithms for LIT

The number of studies investigating the potential of satellite remote sensing data for the estimation of LIT has been limited to date. Kang et al. (2010) first showed brightness temperature (Tb) measurements from the Advanced Microwave Scanning Radiometer for EOS (AMSR-E) at 18.7 GHz frequency (V polarization) to be highly sensitive (R2 = 0.91) to the seasonal evolution of ice thickness on Great Bear Lake (GBL) and Great Slave Lake (GSL), Canada. Based on this finding, Kang et al. (2014) proposed empirical (linear regression) equations to estimate LIT for the two lakes using 18.7 GHz V-pol data (2002-2009), achieving a mean bias error (MBE) of 0.06 m and root mean square error (RMSE) of 0.19 m when compared to in situ measurements. Surface temperature observations of snow-covered lake ice from the Moderate Resolution Imaging Spectroradiometer (MODIS) have also been assessed for the estimation of LIT. Using heat balance terms and snow depth derived from the Canadian Lake Ice Model (CLIMo, Duguay et al. 2003), Kheyrollah et al. (2017) retrieved ice thicknesses up to ~ 1.2 m from MODIS (2002-2014) with an RMSE of 0.17 m and MBE of 0.07 m when comparing LIT values from single pixels (1 km x 1 km) to those from close by near-shore field measurements collected on GSL and Baker Lake, Canada. Beckers et al. 2017 analyzed waveforms from CryoSat2 (CS2) Ku-band synthetic aperture radar (SAR) altimetry for the estimation of LIT on the Great Bear Lake and Great Slave Lake. By exploiting the increasing distance between peak radar returns from the snow-ice and ice-water interfaces on the leading edge of waveforms with ice growth, the authors estimated ice thickness empirically with RMSE < 0.33 m when compared to in situ measurements from the same near-shore location on GSL as in previous investigations. While data from CS2 show strong potential for the retrieval of LIT, the drifting orbit of the satellite makes it difficult to build a geographically precise time series of LIT measurements (i.e., repeated along the same tracks over the lifetime of the satellite) required for climate monitoring. Also, the LIT retracker algorithm developed in Beckers et al. (2017) relies on the empirical thresholding of the radar waveforms that is hard to generalize to follow the LIT evolution, in particular at the seasonal transitions, and can lead to biases and sub-optimal LIT estimates. More recent studies, e.g., Shu et al. (2020), Yang et al. (2021), have estimated LIT with radar altimetry data, more specifically from Sentinel-3 and Jason-3 missions, in the context of lake water level analysis, as the presence of lake ice has been shown to introduce a bias on winter water level measurements. These studies also used empirical methods based on already existing retrackers that are not specifically designed for the estimation of LIT. To overcome these limitations, Mangilli et al. (2022) developed a novel physically-based retracking algorithm, the LRM_LIT retracker, founded on the exploitation of the Ku band radar waveforms data in Low Resolution Mode (LRM) data specifically tailored for the retrieval of LIT. The advantage of a physically-based and analytical retracker is that it does not rely on empirical or by-hand settings, allowing to derive robust and continuous LIT estimates over different target lakes and LRM radar altimetry missions, making the LRM_LIT algorithm the suitable tool to build robust and long LIT timeseries for climate monitoring. The LRM_LIT retacker is the algorithm currently being implemented in the lakes_cci LIT processor.

## 7.2 Future improvements for LIT

The LIT analysis currently scheduled for Phase2 is based on the LRM_LIT algorithm (developed in Phase 1), tailored to detect the LIT signature on the Low Resolution Mode (LRM) Ku band waveforms. While this method provides with a significant improvement with respect to current LIT constraints, the accuracy of the LIT retrievals could be further improved by performing the LIT analysis with Ku radar waveform data at higher resolution, namely, UnFocused SAR andFullyFocused SAR data. This would imply to change the LIT analytical model as the SAR waveforms and the associated LIT signature over iced covered lake is different from the Low Resolution Mode (LRM) waveforms. An R&D study on the development and validation of the analytical based LIT retracker for SAR data (SAR_LIT retracker, Mangilli et al. 2023, in prep.) is ongoing within the S6JTEX ESA project and its use to process SAR data for LIT analysis could be timely to be considered for future improvement of the CCI-Lakes LIT products.

## 7.3 LIT References

K.-K. Kang, C. R. Duguay, S. E. L. Howell, C. Derksen, and R. Kelly, Sensitivity of AMSR-E brightness temperatures to the seasonal evolution of lake ice thickness, IEEE Geoscience and Remote Sensing Letters, vol. 7, no. 4, pp. 751–755, 2010.

K.-K. Kang, C. Duguay, J. Lemmetyinen, and Y. Gel, Estimation of ice thickness on large northern lakes from AMSR-E brightness temperature measurements, Remote Sensing of Environment, vol. 150, pp. 1–19, 2014

H. Kheyrollah Pour, C. R. Duguay, K. A. Scott, and K.- K. Kang, Improvement of Lake Ice Thickness Retrieval From MODIS Satellite Data Using a Thermodynamic Model, IEEE Transactions on Geoscience and Remote Sensing, vol. 55, no. 10, pp. 5956–5965, 2017

Zakharova, E., S. Agafonova, C. Duguay, N. Frolova, and A. Kouraev, 2021. River ice phenology and thickness from satellite altimetry. Potential for climate studies and ice bridge road operation. *The Cryosphere*, 15: 5387-5407, https://doi.org/10.5194/tc-15-5387-2021

J. F. Beckers, J. Alec Casey, and C. Haas, Retrievals of lake ice thickness from Great Slave Lake and Great Bear Lake using CryoSat-2, IEEE Transactions on Geoscience and Remote Sensing, vol. 55, no. 7, pp. 3708–3720, 2017

S. Shu, H. Liu, R. A. Beck, F. Frappart, J. Korhonen, M. Xu, B. Yang, K. M. Hinkel, Y. Huang, and B. Yu, Analysis of Sentinel-3 SAR altimetry waveform retracking algorithms for deriving temporally consistent water levels over ice-covered lakes, Remote Sensing of Environment, vol. 239, p. 111643, 2020

Y. Yang, P. Moore, Z. Li, and F. Li, Lake Level Change From Satellite Altimetry Over Seasonally Ice-Covered Lakes in the Mackenzie River Basin, IEEE Transactions on Geoscience and Remote Sensing, vol. 59, no. 10, pp. 8143–8152, 2021

A. Mangilli, P. Thibaut, C. R. Duguay and J. Murfitt, A New Approach for the Estimation of Lake Ice Thickness From Conventional Radar Altimetry, in IEEE Transactions on Geoscience and Remote Sensing, vol. 60, pp. 1-15, 2022, Art no. 4305515 https://doi.org/10.1109/TGRS.2022.3197109

A. Mangilli, P. Thibaut, C. R. Duguay et al. Improving the Estimation of Lake Ice Thickness with high resolution altimetry data, 2023 in prep.

# Appendix A - List of Acronyms

| | |
|---|---|
| AATSR | Advanced Along Track Scanning Radiometer |
| AATSR | Advanced Along Track Scanning Radiometer |
| AERONET-OC | Aerosol Robotic NETwork – Ocean Color |
| AMI | Active Microwave Instrument |
| AMSR-E | Advanced Microwave Scanning Radiometer for EOS |
| APP | Alternating Polarization mode Precision |
| ASAR | Advanced Synthetic Aperture Radar |
| ASLO | Association for the Sciences of Limnology and Oceanography |
| ATBD | Algorithm Theoretical Basis Document |
| ATSR | Along Track Scanning Radiometer |
| AVHRR | Advanced very-high-resolution radiometer |
| BAMS | Bulletin of the American Meteorological Society |
| BC | Brockman Consult |
| C3S | Copernicus Climate Change Service |
| CCI | Climate Change Initiative |
| CDR | Climate Data Record |
| CDOM | Coloured Dissolved Organic Matter |
| CEDA | Centre for Environmental Data Archival |
| CEMS | Centre for Environmental Monitoring from Space |
| CEOS | Committee on Earth Observation Satellites |
| CGLOPS | Copernicus Global Land Operation Service |
| CIS | Canadian Ice Service |
| CLS | Collecte Localisation Satellite |
| CMEMS | Copernicus Marine Environment Monitoring Service |
| CMUG | Climate Modelling User Group |
| CNES | Centre national d'études spatiales |
| CNR | National Research Council of Italy |
| CORALS | Climate Oriented Record of Altimetry and Sea-Level |
| CPD | Communication Plan Document |
| CR | Cardinal Requirement |
| CRG | Climate Research Group |
| CSWG | Climate Science Working Group |
| CTOH | Center for Topographic studies of the Ocean and Hydrosphere |
| DOC | Dissolved Organic Carbon |
| DUE | Data User Element |
| ECMWF | European Centre for Medium-Range Weather Forecasts |
| ECV | Essential Climate Variable |
| ELLS-IAGRL | European Large Lakes Symposium-International Association for Great Lakes Research |
| ENVISAT | Environmental Satellite |
| EO | Earth Observation |
| EOMORES | Earth Observation-based Services for Monitoring and Reporting of Ecological Status |
| ERS | European Remote-Sensing Satellite |
| ESA | European Space Agency |
| ESRIN | European Space Research Institute |
| ETM+ | Enhanced Thematic Mapper Plus |
| EU | European Union |
| EUMETSAT | European Organisation for the Exploitation of Meteorological Satellites |
| FAQ | Frequently Asked Questions |
| FCDR | Fundamental Climate Data Record |

| | |
|---|---|
| FIDUCEO | Fidelity and Uncertainty in Climate data records from Earth Observations |
| FP7 | Seventh Framework Programme |
| GAC | Global Area Coverage |
| GCOS | Global Climate Observing System |
| GEMS/Water | Global Environment Monitoring System for freshwater |
| GEO | Group on Earth Observations |
| GEWEX | Global Energy and Water Exchanges |
| GloboLakes | Global Observatory of Lake Responses to Environmental Change |
| GLOPS | Copernicus Global Land Service |
| GTN-H | Global Terrestrial Network – Hydrology |
| GTN-L | Global Terrestrial Network – Lakes |
| H2020 | Horizon 2020 |
| HYDROLARE | International Data Centre on Hydrology of Lakes and Reservoirs |
| ILEC | International Lake Environment Committee |
| INFORM | Index for Risk Management |
| IPCC | Intergovernmental Panel on Climate Change |
| ISC | International Science Council |
| ISO | International Organization for Standardization |
| ISRO | Indian Space Research Organisation |
| JRC | Joint Research Centre |
| KPI | Key Performance Indicators |
| LEGOS | Laboratoire d'Etudes en Géophysique et Océanographie Spatiales |
| LIC | Lake Ice Cover |
| LIT | Lake Ice Thickness |
| LSC | Lake Storage Change |
| LSWT | Lake Surface Water Temperature |
| LWE | Lake Water Extent |
| LWL | Lake Water Level |
| LWLR | Lake Water Leaving Reflectance |
| MERIS | MEdium Resolution Imaging Spectrometer |
| MGDR | Merged Geophysical Data Record |
| MODIS | Moderate Resolution Imaging Spectroradiometer |
| MSI | MultiSpectral Instrument |
| MSS | MultiSpectral Scanner |
| NASA | National Aeronautics and Space Administration |
| NERC | Natural Environment Research Council |
| NetCDF | Network Common Data Form |
| NOAA | National Oceanic and Atmospheric Administration |
| NSERC | Natural Sciences and Engineering Research Council |
| NSIDC | National Snow & Ice Data Center |
| NTU | Nephelometric Turbidity Unit |
| NWP | Numerical Weather Prediction |
| OLCI | Ocean and Land Colour Instrument |
| OLI | Operational Land Imager |
| OSTST | Ocean Surface Topography Science Team |
| PML | Plymouth Marine Laboratory |
| PP | Payment Plan |
| PRISMA | PRecursore IperSpettrale della Missione Applicativa |
| Proba | Project for On-Board Autonomy |
| QSR | Quarterly Status Report |
| R | Linear Correlation Coefficient |
| RA | Radar Altimeter |
| RMSE | Root Mean Square Error |

| | |
|---|---|
| SAF | Satellite Application Facility |
| SAR | Synthetic Aperture Radar |
| SeaWIFS | Sea-viewing Wide Field-of-view Sensor |
| SIL | International Society of Limnology |
| SLSTR | Sea and Land Surface Temperature Radiometer |
| SoW | Statement of Work |
| SPONGE | SPaceborne Observations to Nourish the GEMS |
| SRD | System Requirements Document |
| SSD | System Specification Document |
| SST | Sea Surface Temperature |
| STSE | Support To Science Element |
| SWOT | Surface Water and Ocean Topography |
| TAPAS | Tools for Assessment and Planning of Aquaculture Sustainability |
| TB | Brightness Temperature |
| TM | Thematic Mapper |
| TOA | Top Of Atmosphere |
| TR | Technical Requirement |
| UNEP | United Nations Environment Programme |
| UoR | University of Reading |
| UoS | University of Stirling |
| US | United States |
| VIIRS | Visible Infrared Imaging Radiometer Suite |
| WCRP | World Climate Research Program |
| WHYCOS | World Hydrological Cycle Observing Systems |
| WMO | World Meteorological Organization |
| WP | Work Package |